

Regioselective Direct C–H Bond (Hetero)arylation of Thiazoles Enabled by a Novel Iminopyridine-Based α -Diimine Nickel(II) Complex Evaluated by DFT Studies

Phillip Damien E. Arche¹, Shubham Chatterjee¹, Md Muktaadir Talukder¹, Justin T. Miller¹, John Michael O. Cue¹, Chinthaka M. Udamulle Gedara¹, Richard Lord², Michael C. Biewer¹, G. Andrés Cisneros^{1,3*}, and Mihaela C. Stefan^{1*}

¹Department of Chemistry and Biochemistry, University of Texas at Dallas, Richardson, Texas, United States

²Department of Chemistry, Grand Valley State University, Allendale, Michigan, United States

³Department of Physics, University of Texas at Dallas, Richardson, Texas, United States

ABSTRACT: Direct C–H bond arylation is a highly effective method for synthesizing arylated heteroaromatics. This method reduces synthetic steps and minimizes the formation of impurities. We report an air and moisture-stable iminopyridine-based α -diimine nickel (II) complex for direct C5-H bond arylation of thiazole derivatives. Under low catalyst loading and performing the reactions at lower temperatures (80 °C) under aerobic conditions, we produced mono- and diarylated thiazole units. Competition experiments and density functional theory calculations (DFT) revealed that the mechanism of C–H activation in 4-methylthiazole involves electrophilic aromatic substitution.

Keywords: C–H activation, thiazoles, Nickel, DFT, regioselectivity, mechanism

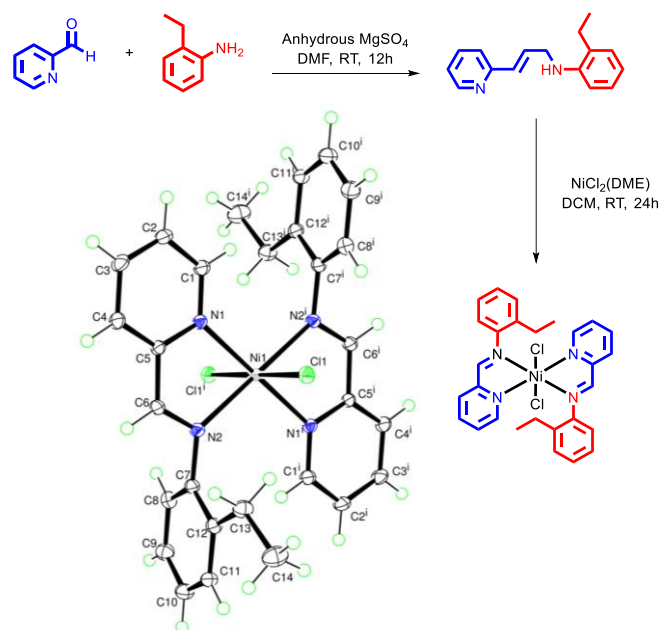
INTRODUCTION

Synthetic organic chemistry has dramatically evolved to create modern synthetic tools for manufacturing valuable (hetero)aryl compounds in organic electronics and drug discovery.¹⁻⁵ Direct C–H bond arylation of heteroaromatics through transition metal catalytic systems has recently drawn significant attention.^{2-3, 6-17} Compared to traditional Negishi, Suzuki, or Stille cross-coupling for making (hetero)aryl compounds, direct arylation offers atom-economical and facile synthetic methods.^{3, 8, 18-19} Consequently, this synthetic tool has emerged as the most desirable technique for synthesizing small molecules, and building blocks containing five-membered heteroaromatics including thiazoles.^{9-10, 18, 20-21} Arylated thiazoles have been cited for using in organic field-effect transistors (OFETs),²² organic solar cells (OSC),²³ and organic light-emitting diodes (OLEDs).⁴ Also, they have manifested promising outcomes in drug discovery and development regarding the structure-activity relationships.^{5, 24-26}

Compared to other transition metal-catalyzed systems, palladium-based systems for direct C–H bond arylation have been extensively studied over the last decade.^{9-10, 20-21, 24-25, 27-39} However, the environmental and financial costs associated with the Pd systems have led the research community to explore more sustainable choices. Accordingly, Ni-based systems are gaining popularity because of their reduced toxicity and cost.⁴⁰⁻⁴³ Nonetheless, many Pd and Ni-catalyzed systems are air- and moisture sensitive.^{17, 24, 29-30, 40-42, 44} Moreover, both Pd and Ni-systems often require *in situ* catalyst generation from expensive precursors.^{29, 31, 41-44} Furthermore, these systems greatly suffer from high catalyst loading (5–10 mol%),^{24-25, 31, 40-42, 44} longer reaction time (12–36 h),^{12-13, 15, 20, 24-25, 27-29, 38-40, 44} high temperature (100–150 °C),^{10-13, 15, 20-21, 24, 27-29, 38-42, 44} and time-consuming ligand synthesis.⁷

Our group has successfully applied α -diimine Ni(II) complexes in Suzuki–Miyaura,⁴⁵ and carbon-sulfur cross-coupling⁴⁶ for synthesizing various building blocks and small molecules. In continuation of our efforts, we report herein the first application of iminopyridine-based α -diimine Ni(II) in

direct C–H bond arylation of thiazole having various reactive functionalities were applied for synthesizing biheteroaryl and π -conjugated poly(hetero)arenes. In an attempt to understand how the nickel catalytic system works on direct arylation of thiazole, DFT calculations were done.



Scheme 1. Synthesis of the α -diimine Ni(II) Complex

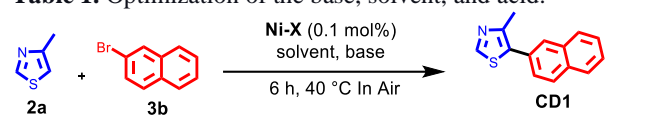
RESULTS AND DISCUSSION

Synthesis and Characterization of α -Diimine Nickel (II) Complex. The synthesis of the complexes and ORTEP diagrams are shown in **Scheme 1**. N-(2-ethylphenyl)-1-(pyridin-2-yl)methanimine (**X**) was synthesized from 2-pyridinecarboxaldehyde and 2-ethylaniline using a previously reported procedure.⁴⁵ For the Ni(II) complex, Ni–**X**, NiCl₂(DME) was reacted with two equivalents of **X**. Ni–

X exhibits a distorted octahedral geometry with two chlorine atoms and four nitrogen atoms from two diamine ligands directly coordinating with the nickel center. No isomers were observed for the crystal structures. Crystal data collection, unit cell representations, selected bond angles, and distances are provided in the supporting information.

Optimization of Reaction Conditions in Direct C–H Bond Arylation. For this purpose, the reaction of 4-methylthiazole (2a), and 2-bromonaphthalene (3b) was analyzed with 0.1 mol% of Ni–X for obtaining the most suitable base, solvent and acid combination at 40 °C for 6 h (Table 1). In the first twelve experiments (Table 1, entries 1–12), we employed pivalic acid (PivOH) and altered the base and solvent to optimize the conditions. Subsequently, an additional two experiments were performed with benzoic acid; however, the yields did not improve for either catalytic system. Ni–X afforded the best yields using K₃PO₄ and DMF (Table 1, entry 2). (See ESI).

Table 1. Optimization of the base, solvent, and acid.^a



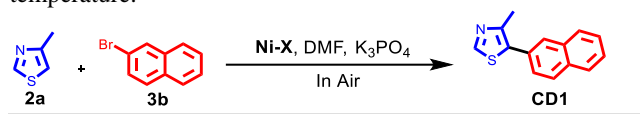
entry	base	solvent	acid	yield (%) ^b
1	K ₂ CO ₃	DMF	PivOH	51
2	K ₃ PO ₄	DMF	PivOH	68
3	NaOH	DMF	PivOH	43
4	K ₂ CO ₃	H ₂ O	PivOH	34
5	K ₃ PO ₄	H ₂ O	PivOH	40
6	NaOH	H ₂ O	PivOH	57
7	K ₂ CO ₃	MeCN	PivOH	58
8	K ₃ PO ₄	MeCN	PivOH	42
9	NaOH	MeCN	PivOH	19
10	K ₂ CO ₃	1,4-dioxane	PivOH	53
11	K ₃ PO ₄	1,4-dioxane	PivOH	47
12	NaOH	1,4-dioxane	PivOH	56
13	K ₃ PO ₄	DMF	PhCOOH	53
14	NaOH	MeCN	PhCOOH	48

^aReaction conditions: 4-methylthiazole (1.5 mmol), 2-bromonaphthalene (1 mmol), base (1.5 mmol), 0.1 mol% of Ni–X, solvent (6 mL), PivOH (0.2 mmol) for 6 h at 40 °C under aerobic conditions. ^bYields as isolated from column chromatography.

Another set of experiments was carried out to optimize the reaction time, temperature, and catalyst loading (Table 2). Keeping the catalyst loading at 0.1 mol%, three experiments were performed at 60, 80, and 100 °C for six hours (Table 2, entries 1–3). The yields for Ni–X increased by raising the temperature from 40 to 80 °C; however, they decreased at 100 °C (Table 2, entries 1–3). Increasing the catalyst loading to 0.3 mol% did not improve the yield for Ni–X (Table 2, entry 5). Variations on reaction time were performed for Ni–X, and the optimal reaction time was six hours. Ultimately, the best yields were recorded using catalyst loading of 0.2 mol% for six hours at 80 °C (Table 2, entry 8). No background reactivity was

observed without employing the synthesized Ni complex/ligands under the used conditions.

Table 2. Optimization of time, concentration of complex, and temperature.^a



entry	time	Ni–X (mol%)	temp (°C)	yield (%) ^b
1	6	0.1	60	76
2	6	0.1	80	85
3	6	0.1	100	78
4	6	0.2	80	91
5	6	0.3	80	82
6	8	0.2	80	78
7	4	0.2	80	80
8	6	0	80	0

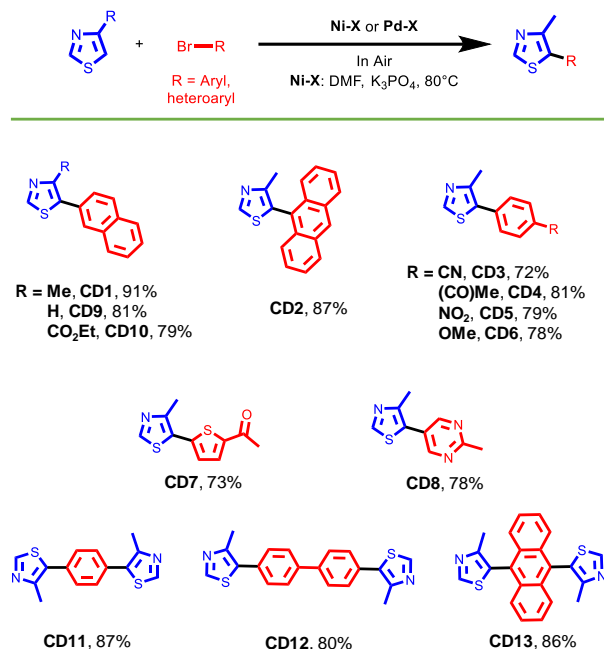
^aReaction conditions: 4-methylthiazole (1.5 mmol), 2-bromonaphthalene (1 mmol), base (1.5 mmol), Ni–X, solvent (6 mL), and PivOH (0.2 mmol) under aerobic conditions. ^bYields as isolated from column chromatography.

Evaluation of catalytic performance. Arylated thiazoles are essential building blocks found in biologically active natural products, drug molecules, agrochemicals, and novel optical materials.^{24–25} Here, 12 compounds with thiazole units were synthesized applying the optimized reaction conditions (Scheme 2). Different aryl and heteroaryl bromides, including nitrile, acetyl, nitro, and alkoxy functionalities, were introduced for making the heteroaryl or biheteroaryl compounds. Activation of the catalytic systems on aryl dibromides was also applied to a couple with two units of thiazole. Sterics, at least in the case of introducing bulky naphthalene and anthracene units for making the compound CD1 and CD2 (Scheme 2), was not observed as a problem in direct arylation. In terms of electronics, both the electron-donating group (EDG) and electron-withdrawing group (EWG) on the aryl halide, as well as heteroaryl halide, were tolerated (CD3 to CD8). We tried applying the optimized reaction conditions to thiazole (2b) and ethyl thiazole-4-carboxylate (2c), but CD11 and CD12 were formed at 100 °C for 12 h and 24 h, respectively. The decrease in the activity of the catalytic reaction conditions prompted us to continue the substrate scope with the direct arylation of 4-methylthiazole.

Pi-conjugated poly(hetero)arenes are widely studied functional materials for electrochromic and optoelectronic device fabrication.⁴⁸ Here, we have explored our catalytic systems to synthesize π -conjugated poly(hetero)aryl compounds through double direct C–H bond arylation of aryl bromides (CD11 to CCD13). Anthracene is a valuable supramolecular building block that provides a low electronic bandgap in OLED applications.⁴⁹ The bulky anthracene unit was successfully incorporated to form CD13. Thiazoles prefer direct arylation on C2 and C5 positions.⁷¹ Regarding these optimized conditions, we only observed the C5 selectivity of thiazole derivatives upon direct C–H bond heteroarylation (see

Figure S14 in SI), as observed in other studies, including the electrophilic palladation at C5 of thiazoles.^{17,26,29-31}

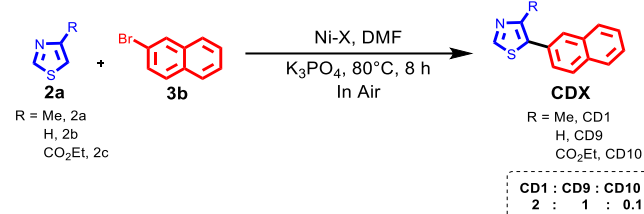
Scheme 2. Evaluation of catalytic performance.^a



^aHeteroaryl (1.5 mmol), halide (1 mmol), DMF (6 mL), K₃PO₄ (1.5 mmol), 0.2 mol% of Ni-X, PivOH (0.2 mmol) for six hours at 80 °C. Yields as isolated from column chromatography.

Competition Experiment. In the electrophilic metallation, the transition metal attacks the most nucleophilic site of the arene, resulting in the Wheland σ -complex⁷². Carbocationic in nature of the Wheland σ -complex can be hastened by EDG and suppressed by (EWG) at C4 of thiazole derivatives in this case because the former provides more stability similar to an electrophilic aromatic substitution EAS. A competition study⁷³ was then conducted among **2a**, **2b**, and **2c** to support whether electrophilic metallation occurs in the nickel-catalyzed direct arylation procedure presented. The kinetics experiment resulted in relative rates of **2:1:0.1** for **CD1:CD9:CD10**. These results show that arylation is the fastest using **2a** (with EDG) and the slowest with **2c** (with EWG) at C4, which suggests the possibility of electrophilic addition as the mechanism involved.

Scheme 3. Competition experiment.



Mechanistic Studies of C–H activation in 4-methylthiazole using DFT Calculations: We investigated the energy required for pre-activation of iminopyridine-based α -diimine nickel(II) (Ni-X) by two main possible pathways: a) Ni⁰/Ni^{II}-based pathway and

b) Ni^{II}/Ni^{IV} pathway. Under the Ni⁰/Ni^{II}-based pathway, we explored the possibility of removing the usually labile chloride ligands as Cl₂ to generate Ni⁰-AC^A, referred as the (Ni⁰/Ni^{II} (A) mechanism in **Figure 1**). Our calculations suggest that a pre-activation energy of 60.3 kcal mol⁻¹ is required to form Ni⁰-AC^A from Ni-X. Thus, this pathway was deemed unfeasible. The corresponding reaction energy profile and cartesian coordinates of the calculated intermediates and transition states for Ni⁰/Ni^{II} (A) are provided in the SI.

Next, for the Ni^{II}/Ni^{IV} based pathway, there are two possibilities for the pre-activation. First, we tested a mechanism where Ni-X loses the two chloride ligands as chloride ions (termed Ni^{II}/Ni^{IV} (B) mechanism, **Figure 1**) with Ni^{II}-AC^B as an active catalyst. Alternately, we tested the formation of Brookhart-type α -diimine nickel (II) active-catalyst (Ni^{II}-AC^C) (termed Ni^{II}/Ni^{IV} (C) mechanism, **Figure 1**). Our results indicate that the Ni^{II}-AC^B based mechanism requires 21.4 kcal mol⁻¹ to form the active catalyst, whereas the Ni^{II}-AC^C results in uphill energy of 7.9 kcal mol⁻¹ compared with Ni-X. Thus, the Ni^{II}/Ni^{IV} (B) mechanism was also deemed unfeasible and will not be considered for further calculations. The detailed investigation of the subsequent steps in the Ni^{II}/Ni^{IV} (C) mechanism with Ni^{II}-AC^C as the active catalyst was explored further based on the initial catalyst activation. The relative zero-point-corrected energies (ΔE in kcal mol⁻¹) calculated with PBE0-D3(BJ)/def2-TZVP (SMD: DMF) level of theory and structures for the proposed mechanism are shown in **Figure 2**, setting the Ni^{II}-AC^C structure as the reference (0.0 kcal mol⁻¹). The proposed mechanism is a combination of three processes, namely, the oxidative addition of 2-bromonaphthalene onto the Ni^{II}-AC^C complex, the C–H bond activation in **2a**, and last, a reductive elimination to form the arylated **2a**. The calculated reaction profile connecting the minimum energy structures for the lowest energy mechanism is presented in **Figure 2**.

Oxidative Addition. The reaction proceeds with the oxidative addition of 2-bromonaphthalene starting from the Ni^{II}-AC^C active catalysis, which adopts a distorted square planar geometry. The C α -Br bond in **3b** is activated via transition state **TS-OA** by overcoming an activation barrier of 28.6 kcal mol⁻¹. The cleavage of the C α -Br bond leads to the formation of Ni(IV) complex (**IM1**) with a reaction energy of 14.5 kcal mol⁻¹. Analysis of the electronic structures of Ni^{II}-AC^C and **IM1** to determine the oxidation states in these complexes is presented in the SI (**Tables S5** and **S6**).

C–H Bond Activation. A ligand exchange between the Br⁻ anion and the PivO⁻ anion further leads to a highly exergonic process forming **IM2** (-12.2 kcal mol⁻¹). In the subsequent step, 4-methylthiazole reacts with the **IM2** to replace the pivalate ligand. The nickel catalyst acts as an electrophile, and there are two potential nucleophilic sites, i.e., C2 and C5, on **2a**. We investigated the pathways associated with the attack of the nickel catalyst as an electrophile on **2a** at C2 (Pathway C2, in violet) and C5 (Pathway C5, in green) sites. Next, the electrophilic attack on **2a** produces the linkage isomers **IM3(C2)** and **IM3(C5)** along Pathway C2 and Pathway C5, respectively. These isomers resemble the Wheland σ -complexes. **IM3(C5)** is 4.5 kcal mol⁻¹ more stable than **IM3(C2)**. Analysis of the electronic structures (**Tables S5**, and **S6**) of **IM3(C2)** and **IM3(C5)** complexes is presented in the SI.

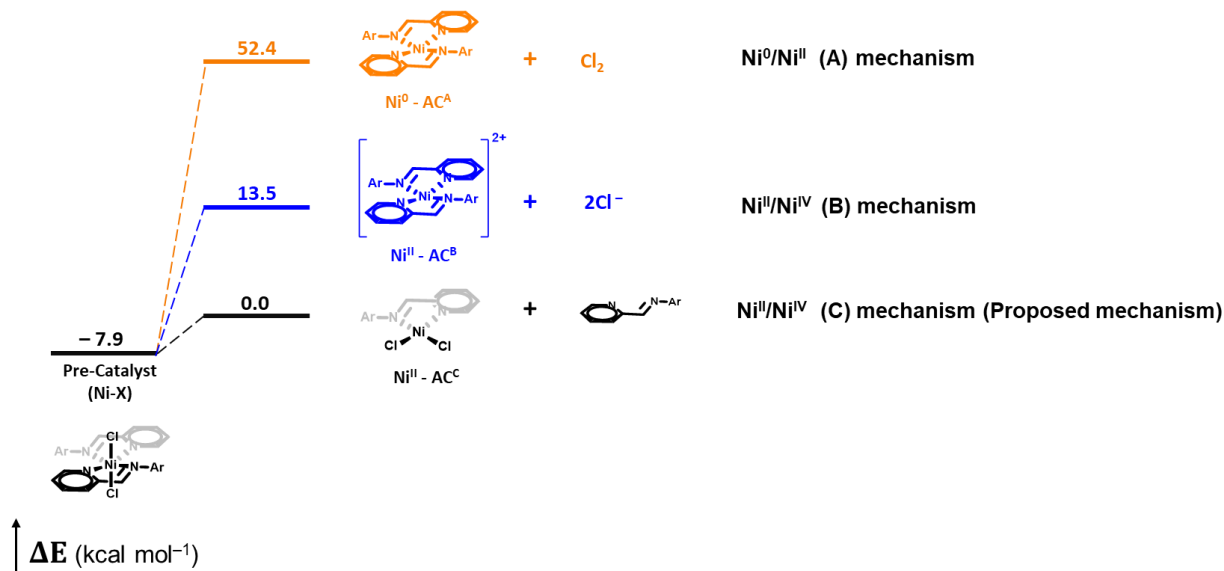


Figure 1. Relative zero-point corrected pre-activation energy calculated with PBE0-D3(BJ)/def2-TZVP (SMD: DMF) level of theory (in kcal mol⁻¹), associated with Ni⁰/Ni^{II} (A) mechanism (in orange), Ni^{II}/Ni^{IV} (B) (in blue), and Ni^{II}/Ni^{IV} (C) (in black) mechanisms.

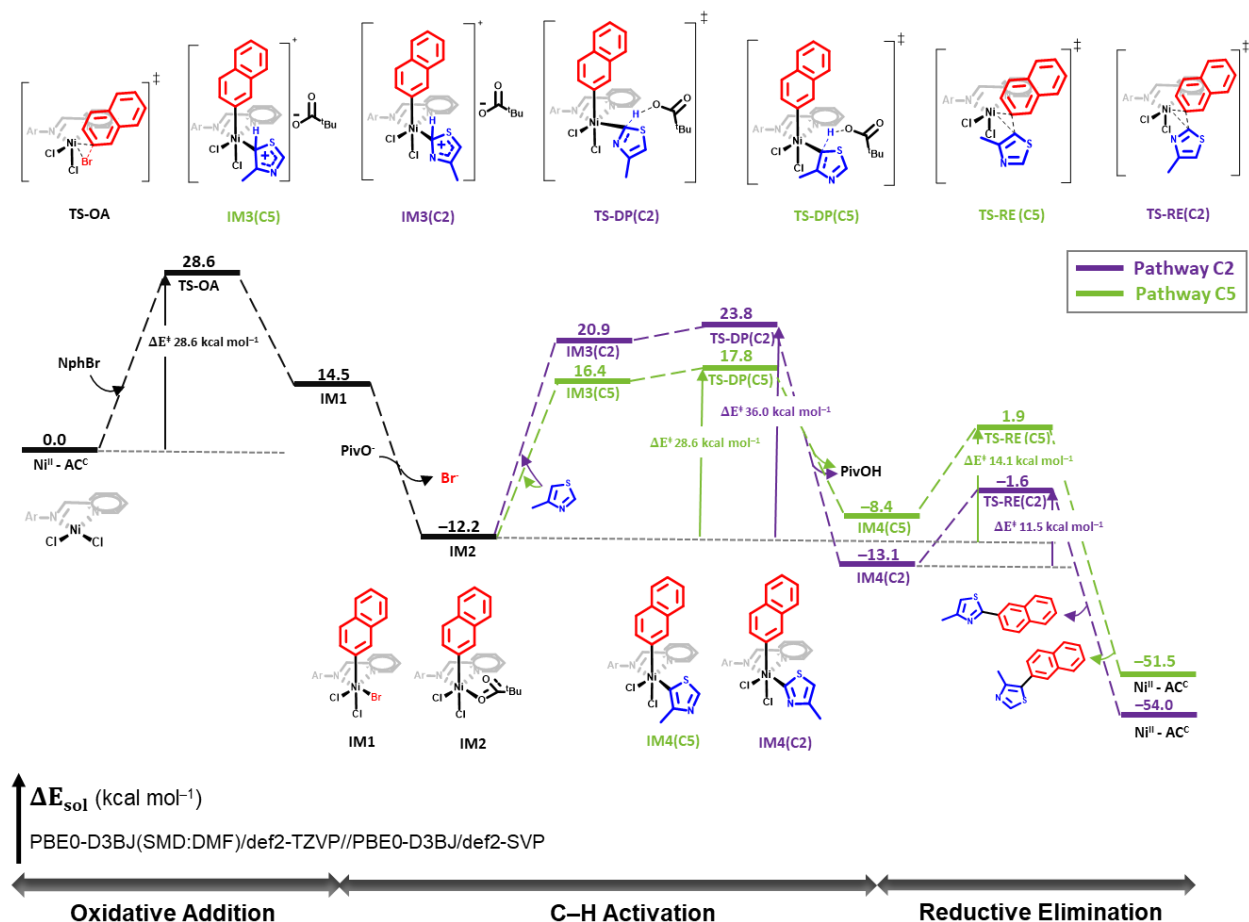


Figure 2. Calculated reaction energy (kcal mol⁻¹) profile for the direct C-H bond arylation of 2a following the Ni^{II}/Ni^{IV} mechanism. Pathway C2 (in violet) and Pathway C5 (in green) show C2 and C5 activation pathways, respectively.

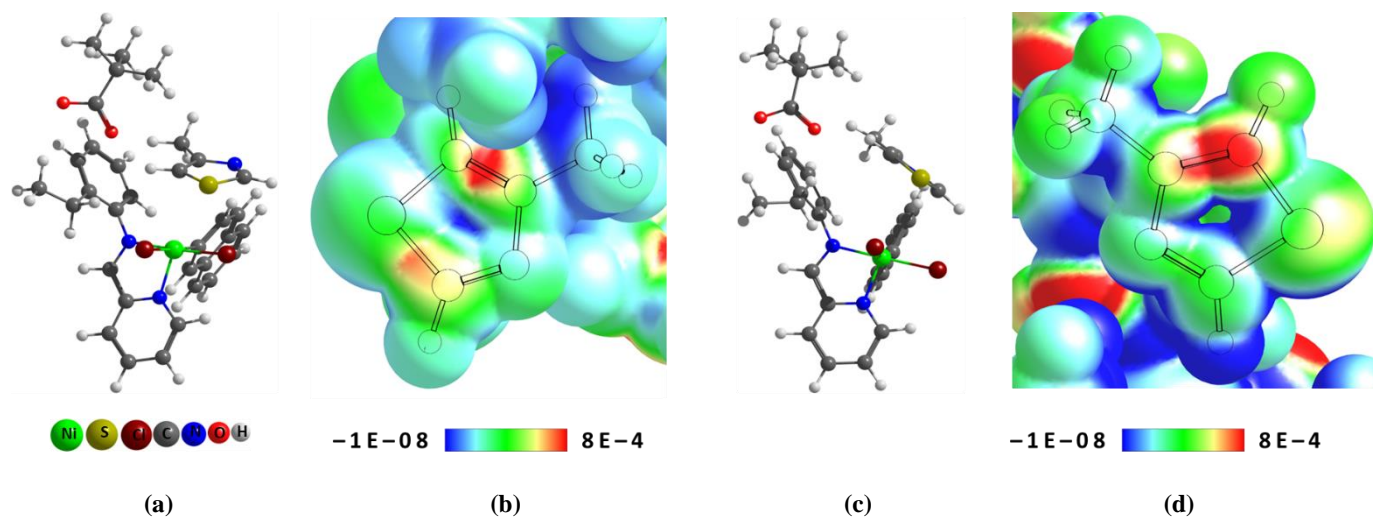


Figure 3. Optimized structure representing the initial part of the reaction of **2a** with the nickel-catalyst for the formation of **IM3(C2)** (a), electron donor Fukui function, $f^-(r)$, on 0.001 a.u. electron density isosurface for **2a** in (a) (b), Optimized structure representing the initial part of the reaction of thiazole with the nickel-catalyst for the formation of **IM3(C5)** (c), and electron donor Fukui function, $f^-(r)$, on 0.001 a.u. electron density isosurface for **2a** in (c) (d).

In the next step, the proton can be abstracted by **PivO⁻** from either C2 or C5. The deprotonation proceeds through an electrophilic aromatic substitution mechanism involving transition states **TS-DP(C2)** along Pathway C2 and **TS-DP(C5)** along Pathway C5. **TS-DP(C5)** is 6.0 kcal mol⁻¹ more stable than **TS-DP(C2)**. The energy diagram indicates that an electrophilic attack by the nickel catalyst over C5 is kinetically favored over an attack on C2. The deprotonation leads to intermediates **IM4(C2)** and **IM4(C5)**, where **IM4(C2)** is more stable than **IM4(C5)** by 4.7 kcal mol⁻¹. The deprotonation step remains the rate-determining step for both pathways, with barrier heights of 36.0 kcal mol⁻¹ and 30.0 kcal mol⁻¹ for Pathway C2 and Pathway C5, respectively.

The local electrophilicity of **2a** can be investigated using a Fukui function analysis. The Fukui function is a useful DFT local reactivity descriptor. It has been used in several previous studies,⁵⁰⁻⁵⁴ especially for systems that involve intermolecular electron exchange reactions. We investigated the distribution of the electron donor Fukui function for **2a** in the presence of the nickel catalyst and **PivO⁻** (Figure 3) in two different orientations corresponding to the initial steps of the reaction between 4-methylthiazole and the nickel catalyst for the formation of **IM3(C2)** and **IM3(C5)** (see Figure 3, (a) and (c)). Figures 3 (b) and (d) show the distribution of values of the electron donor Fukui function $f^-(r)$ on 0.001 a.u. electron density isosurface for both structures. Figures 3 (b) and (d) indicate that C5 is a preferred site for an electrophilic attack than C2.

Reductive Elimination. The final step corresponds to reductive elimination. **IM4(C2)** and **IM4(C5)** produce the heteroarylation products via transition states **TS-RE(C2)** and **TS-RE(C5)**, respectively. **TS-RE(C2)/TS-RE(C5)** involves the formation of the C–C bond between the C2/C5 of **2a** and C α of the naphthalene ligand. The reaction barriers for **TS-RE(C2)/TS-RE(C5)** are 11.5 kcal mol⁻¹ and 10.3 kcal mol⁻¹ with respect to intermediates **IM4(C2)/IM4(C5)**. Finally, after the C–C bond formations, the **CD1** is released, coupled with the regeneration of Ni^{II}–AC. Both processes are endothermic with

the release of 52.4/53.4 kcal mol⁻¹ along Path C2/Path C5 with respect to **TS-RE(C2)/TS-RE(C5)**. Based on our calculations, the reaction energy profile suggests that the primary product for the reaction of **2a** and **3b** is **CD1** formed along Path C5.

CONCLUSIONS

In summary, we have created a Ni-catalytic system that utilizes an iminopyridine-based α -diimine Ni(II) complex. This system enables the direct C–H bond arylation of multiple thiazole derivatives, even under low-temperature aerobic conditions and with a catalyst loading as low as 0.1 mol%. Our catalytic system selectively arylates the C5 position of thiazoles to generate heteroaryl compounds with diverse reactive functionalities. We investigated the underlying mechanism of this selectivity by carrying out a competition experiment, which showed that the reaction was accelerated by electron-donating groups (EDGs) on thiazole. In contrast, electron-withdrawing groups (EWGs) delayed the reaction. The study found that the direct reaction between 4-methylthiazole and 2-bromonaphthalene has a high yield of 91% when using specific reaction conditions (80 °C temperature, air, and DMF as the solvent). As a result, we conducted a thorough mechanistic study using DFT-based methods to investigate the direct C2–H /C5–H bond arylation of 4-methylthiazole using an iminopyridine-based α -diimine nickel(II) complex. The possible pathways for C5–H with Ni^{II}–AC^c as the active catalyst for C2–H /C5–H bond activation were explored, and we compared the corresponding rate-determining steps. The reaction mechanisms comprised three major processes: oxidative addition, C2–H /C5–H bond activation, and reductive elimination. The formation of the rate-determining TS for the formation of the 4-methyl-2-(naphthalen-2-yl)thiazole via C2 atom activation was found to be higher in energy than that of C5, which indicates higher regioselectivity of the catalyst towards C5 atom of 4-methylthiazole, and a higher yield of the final product, i.e., 4-methyl-5-(naphthalen-2-yl)thiazole. This prediction is consistent with the experimentally observed results. Further, the analysis of the condensed Fukui function of

4-methylthiazole provided further insights on the mechanism and indicated a more facile electrophilic attack over C5 than that over C2 of 4-methylthiazole, by the nickel catalyst.

GENERAL MATERIALS AND METHODS

Experimental methods: All reagents were purchased from Sigma-Aldrich or Fisher Scientific and employed without additional purification unless otherwise specified. ^1H NMR and ^{13}C NMR spectra were collected using a 500 MHz Bruker AVANCE III spectrometer with chloroform as the reference solvent. Synthesized α -diimine complexes were characterized by elemental analysis using a Thermo FLASH 2000 CHN elemental analyzer. For collecting the MS (EI) data, a Waters ACQUITY UPLC M-Class was employed. All the reactions except for the synthesis of the α -diimine complexes were performed in the air atmosphere.

Single-Crystal XRD Data Characterization. A Bruker Kappa D8 Quest CPAD diffractometer equipped with an Incoatec microfocus Mo $K\alpha$ radiation source, Oxford Cryosystems cooler, and Photon 100 CMOS detector ($\lambda = 0.71073 \text{ \AA}$) was utilized for acquiring the single-crystal X-ray diffraction data. Bruker APEX3 graphical interface and Bruker SAINT were applied to achieve data reduction and cell refinement. Moreover, Bruker XPREP and SADABS were used to estimate the space group and multi-scan absorption correction, respectively. To solve and refine the structure, SHELXTL (intrinsic phasing method)⁶⁹ and SHELXL2017⁷⁰ were applied, respectively. The publCIF and ORTEP-3 were used for the preparation of the crystallographic Information File (CIF).

Synthesis of Iminopyridine Ligand *N*-(2-ethylphenyl)-1-(pyridin-2-yl)methanimine (X). The ligand X was synthesized by adopting a previously published procedure.⁴⁵ In a one-neck 100 mL flask, 2-pyridinecarboxaldehyde (3.0 mL, 0.032 mol) and 2-ethylaniline (3.88 g, 0.032 mol) were mixed with anhydrous MgSO_4 (120 mg, 1 mmol), and DMF (40 mL) as a solvent. The reaction mixture was stirred for ten hours at room temperature. After that, three extractions were performed with 40 mL of ethyl acetate and 40 mL of distilled water. After drying the ethyl acetate layer with anhydrous MgSO_4 , the crude product was obtained by concentrating with the rotary evaporator. The final pure product was collected by employing silica gel column chromatography using *n*-hexane as an eluent. The product was isolated as dark-orange oil (Yield = 5.24 g, 77.9%). MS (EI) m/z $[\text{M} + \text{H}]^+ = 211.0104$ (calculated for $\text{C}_{14}\text{H}_{14}\text{N}_2$, 211.0139). ^1H NMR (500 MHz, CDCl_3 , 300 K): δ (ppm): 8.70 (d, $J = 4.15 \text{ Hz}$, 1H), 8.55 (s, 1H), 8.25 (d, $J = 7.85 \text{ Hz}$, 1H), 7.78 (t, $J = 7.65 \text{ Hz}$, 1H), 7.34 (t, $J = 6.05 \text{ Hz}$, 1H), 7.19 – 7.27 (m, 3H), 7.02 (d, $J = 7.35 \text{ Hz}$, 1H), 2.83 (q, $J = 7.45 \text{ Hz}$, 2H), 1.22 (t, $J = 7.55 \text{ Hz}$, 3H).

Synthesis of the Iminopyridine Bis-Ligated Nickel(II) Complex (Ni-X). Complex Ni-X was synthesized by adopting a previously published procedure.⁴⁵ $\text{NiCl}_2(\text{DME})$ (219.72 mg, 1 mmol) was transferred to a one-neck 50 mL flask having a magnetic stirrer. The flask was purged with nitrogen before adding the ligand 2-ethyldiimine (420.56 mg, 2 mmol) dissolved in dichloromethane (20 mL). After stirring at room temperature for 24 hours, the precipitated solid was filtered and washed with petroleum ether (40 mL) and hexane (40 mL). The pure product was isolated as a light green solid after drying under vacuum for 24 hours (Yield = 480.17 mg, 87.3%).

Elemental analysis: calculated for $\text{C}_{28}\text{H}_{28}\text{Cl}_2\text{N}_4\text{Ni}$: C, 61.13; H, 5.13; N, 10.18. Found: C, 61.23; H, 5.01; N, 10.27. Acetonitrile was used as a solvent for growing the single crystal for XRD analysis. A saturated solution of the complex was formed, and it was slowly evaporated over one week. Crystal size: $0.18 \times 0.16 \times 0.16 \text{ mm}^3$; crystal shape: fragment; crystal color: yellow.

General Procedure for Nickel-Catalyzed Direct Arylation. All the reactions were performed in the air atmosphere. A 25 mL one-neck round bottom flask was equipped with a condenser. For the single direct arylation, the reaction setup was maintained with heteroaryl derivative (1.5 mmol), aryl bromide (1 mmol), DMF (6 mL), K_3PO_4 (1.5 mmol), 0.2 mol% of Ni-X, and PivOH (0.2 mmol). The reaction mixture was stirred for six hours at 80 °C. For the double Direct arylation with bis-halogenated aromatics, the reaction setup was maintained with heteroaryl derivative (2.5 mmol), aryl bromide (1 mmol), DMF (6 mL), K_3PO_4 (3 mmol), 0.4 mol% of Ni-X, and PivOH (0.4 mmol). The reaction mixture was stirred for six hours at 80 °C. For the double direct arylation with mono-halogenated aromatics, the reaction setup was maintained with heteroaryl derivative (1 mmol), aryl bromide (2.5 mmol), DMF (6 mL), K_3PO_4 (3 mmol), 0.4 mol% of Ni-X, and PivOH (0.4 mmol). The reaction mixture was stirred for six hours at 80 °C. After that, the reaction mixture was cooled to room temperature, and it was poured into a 100 mL beaker containing 40 mL of water. Three extractions were carried out with 20 mL of ethyl acetate and 20 mL of distilled water. The ethyl acetate layer was dried over anhydrous MgSO_4 and concentrated through rotary evaporation to obtain the crude product. The pure product was obtained by either precipitation or using silica gel (200–300 mesh) column chromatography.

4-methyl-5-(naphthalen-2-yl)thiazole (CD1). Purified via silica gel column chromatography using *n*-hexane and ethyl acetate as eluents in a ratio of 10:1 (v/v). Colorless oil. Yield: 205.1 mg, 91%. MS (EI) m/z $[\text{M} + \text{H}]^+ = 226.0121$ (calculated for $\text{C}_{14}\text{H}_{11}\text{NS}$, 226.0187). ^1H NMR (500 MHz, CDCl_3 , 300 K): δ (ppm): 8.73 (s, 1H), 7.91 – 7.86 (m, 4H), 7.56 – 7.51 (m, 3H), 2.61 (s, 3H). ^{13}C NMR (500 MHz, CDCl_3 , 300 K), δ (ppm): 150.56, 148.85, 133.32, 132.71, 132.08, 129.42, 128.48, 128.40, 128.07, 127.80, 127.16, 126.76, 126.61, 30.93. ^1H and ^{13}C NMR spectra are consistent with previous reports.⁴⁷

5-(anthracen-9-yl)-4-methylthiazole (CD2). Purified via silica gel column chromatography using *n*-hexane and ethyl acetate as eluents in a ratio of 10:1 (v/v). Light yellow solid. Yield: 239.5 mg, 87%. MS (EI) m/z $[\text{M} + \text{H}]^+ = 276.0219$ (calculated for $\text{C}_{18}\text{H}_{13}\text{NS}$, 276.0226). ^1H NMR (500 MHz, CDCl_3 , 300 K): δ (ppm): 9.03 (s, 1H), 8.57 (s, 1H), 8.06 (d, $J = 8 \text{ Hz}$, 2H), 7.66 (d, $J = 8.5 \text{ Hz}$, 2H), 7.51 – 7.44 (m, 4H), 2.16 (s, 3H). ^{13}C NMR (500 MHz, CDCl_3 , 300 K), δ (ppm): 152.99, 152.55, 131.84, 131.44, 128.80, 128.76, 126.60, 125.93, 125.92, 124.67, 15.50.

4-(4-methylthiazol-5-yl)benzonitrile (CD3). Purified via silica gel column chromatography using *n*-hexane and ethyl acetate as eluents in a ratio of 10:1 (v/v). Light brown oil. Yield: 144.02 mg, 72% (Ni X-1). MS (EI) m/z $[\text{M} + \text{H}]^+ = 201.0101$ (calculated for $\text{C}_{11}\text{H}_8\text{N}_2\text{S}$, 201.0069). ^1H NMR (500 MHz, CDCl_3 , 300 K): δ (ppm): 8.74 (s, 1H), 7.69 (d, $J = 10 \text{ Hz}$, 2H), 7.54 (d, $J = 5 \text{ Hz}$, 2H), 2.55 (s, 3H). ^{13}C NMR (500 MHz, CDCl_3 , 300 K), δ (ppm): 151.63, 150.08, 136.90, 132.56,

130.17, 129.77, 118.50, 111.58, 16.39. ¹H and ¹³C NMR spectra are consistent with previous reports.³⁸

1-(4-(4-methylthiazol-5-yl)phenyl)ethan-1-one (CD4). Purified via silica gel column chromatography using *n*-hexane and ethyl acetate as eluents in a ratio of 10:1 (v/v). Light yellow oil. Yield: 154.11 mg, 71%. MS (EI) *m/z* [M + H]⁺ = 218.0109 (calculated for C₁₂H₁₁NOS, 218.0127). ¹H NMR (500 MHz, CDCl₃, 300 K): δ (ppm): 8.70 (s, 1H), 7.97 (d, *J* = 5 Hz, 2H), 7.50 (d, *J* = 10 Hz, 2H), 2.59 (s, 3H), 2.54 (s, 3H). ¹³C NMR (500 MHz, CDCl₃, 300 K), δ (ppm): 197.28, 151.17, 149.59, 136.83, 136.22, 130.90, 129.29, 128.77, 26.64, 16.38. ¹H and ¹³C NMR spectra are consistent with previous reports.³⁸

5-(4-methoxyphenyl)-4-methylthiazole (CD6). Purified via silica gel column chromatography using *n*-hexane and ethyl acetate as eluents in a ratio of 10:1 (v/v). Light yellow solid. Yield: 135.33 mg, 66%. MS (EI) *m/z* [M + H]⁺ = 206.0119 (calculated for C₁₁H₁₁NOS, 206.0126). ¹H NMR (500 MHz, CDCl₃, 300 K): δ (ppm): 8.50 (s, 1H), 7.24 (d, *J* = 5 Hz, 2H), 6.84 (d, *J* = 10 Hz, 2H), 3.71 (s, 3H), 2.39 (s, 3H). ¹³C NMR (500 MHz, CDCl₃, 300 K), δ (ppm): 159.33, 149.64, 147.85, 131.69, 130.46, 124.12, 114.12, 55.25, 15.93. ¹H and ¹³C NMR spectra are consistent with previous reports.²⁴

4-methyl-5-(2-methylpyrimidin-5-yl)thiazole (CD8). Purified via silica gel column chromatography using *n*-hexane and ethyl acetate as eluents in a ratio of 10:1 (v/v). Colorless oily liquid. Yield: 139.46 mg, 73%. MS (EI) *m/z* [M + H]⁺ = 192.0128 (calculated for C₉H₉N₃S, 192.0113). ¹H NMR (500 MHz, CDCl₃, 300 K): δ (ppm): 8.77 (s, 1H), 8.70 (s, 2H), 2.77 (s, 3H), 2.52 (s, 3H). ¹³C NMR (500 MHz, CDCl₃, 300 K), δ (ppm): 167.55, 156.51, 151.89, 150.78, 124.65, 123.64, 25.89, 15.99.

1-(5-(4-methylthiazol-5-yl)thiophen-2-yl)ethan-1-one (CD7). Purified via silica gel column chromatography using *n*-hexane and ethyl acetate as eluents in a ratio of 10:1 (v/v). Light brown solid. Yield: 173.94 mg, 78%. MS (EI) *m/z* [M + H]⁺ = 224.0135 (calculated for C₁₀H₉NOS₂, 224.0117). ¹H NMR (500 MHz, CDCl₃, 300 K): δ (ppm): 8.65 (s, 1H), 7.60 (d, *J* = 4 Hz, 1H), 7.12 (d, *J* = 4 Hz, 1H), 2.63 (s, 3H), 2.53 (s, 3H). ¹³C NMR (500 MHz, CDCl₃, 300 K), δ (ppm): 190.43, 151.09, 150.81, 144.20, 141.83, 132.85, 127.55, 125.16, 26.65, 17.03.

4-methyl-5-(4-nitrophenyl)thiazole (CD5). Purified via silica gel column chromatography using *n*-hexane and ethyl acetate as eluents in a ratio of 10:1 (v/v). Colorless oil. Yield: 167.22 mg, 76%. MS (EI) *m/z* [M + H]⁺ = 221.0121 (calculated for C₁₀H₈N₂O₂S, 221.0167). ¹H NMR (500 MHz, CDCl₃, 300 K): δ (ppm): 8.76 (s, 1H), 8.25 (d, *J* = 10 Hz, 2H), 7.59 (d, *J* = 10 Hz, 2H), 2.57 (s, 3H). ¹³C NMR (500 MHz, CDCl₃, 300 K), δ (ppm): 151.89, 150.46, 147.14, 138.88, 129.87, 129.81, 124.09, 16.48. ¹H and ¹³C NMR spectra are consistent with previous reports.²⁸

5-(naphthalen-2-yl)thiazole (CD9). Purified via silica gel column chromatography using *n*-hexane and ethyl acetate as eluents in a ratio of 10:1 (v/v). Yellow solid. Yield: 166.9 mg, 79%. GC-MS *m/z* [M + H]⁺ = 192.0128 (calculated for C₉H₉N₃S, 192.0113). ¹H NMR (500 MHz, CDCl₃, 300 K): δ (ppm): 8.85 (s, 1H), 8.25 (s, 1H), 8.07 - 7.87 (m, 4H), 7.75 - 7.53 (m, 3H). ¹³C NMR (500 MHz, CDCl₃, 300 K), δ (ppm): 152.73, 139.84, 133.98, 133.56, 129.40, 128.97, 128.53,

128.27, 127.35, 127.05, 126.40, 125.22. ¹H and ¹³C NMR spectra are consistent with previous reports.⁷⁴

4-ethyl-5-(naphthalen-2-yl)thiazole carboxylate (CD10). Purified via silica gel column chromatography using *n*-hexane and ethyl acetate as eluents in a ratio of 10:1 (v/v). Yellow solid. Yield: 84.99 mg, 30%. MS (EI) *m/z* [M + H]⁺ = 226.0121 (calculated for C₁₄H₁₁NS, 226.0187). ¹H NMR (500 MHz, CDCl₃, 300 K): δ (ppm): 8.82 (s, 1H), 7.86 - 7.91 (m, 4H), 7.61 - 7.53 (m, 3H), 4.32 (q, 2H), 1.25 (t, 3H). ¹³C NMR (500 MHz, CDCl₃, 300 K), δ (ppm): 164.26, 161.98, 151.44, 147.75, 147.48, 141.38, 133.40, 132.74, 132.97, 129.52, 128.59, 127.79, 127.51, 127.08, 126.72, 61.42, 14.13.

1,4-bis(4-methylthiazol-5-yl)benzene (CD11). Pure product was obtained by precipitation method. *n*-hexane was added to a concentrated dichloromethane solution followed by filtering and washing with *n*-hexane. Light red solid. Yield: 236.67 mg, 87%. MS (EI) *m/z* [M + H]⁺ = 273.0112 (calculated for C₁₄H₁₂N₂S₂, 273.0147). ¹H NMR (500 MHz, CDCl₃, 300 K): δ (ppm): 8.70 (s, 2H), 7.50 (s, 4H), 2.58 (s, 6H). ¹³C NMR (500 MHz, CDCl₃, 300 K), δ (ppm): 150.64, 149.00, 131.71, 131.36, 129.62, 16.32. ¹H and ¹³C NMR data are consistent with the reported literature.¹⁵

4,4'-bis(4-methylthiazol-5-yl)-1,1'-biphenyl (CD12). Pure product was obtained by precipitation method. *n*-hexane was added to a concentrated dichloromethane solution followed by filtering and washing with *n*-hexane. Light red solid. Yield: 278.46 mg, 80%. MS (EI) *m/z* [M + H]⁺ = 349.0061 (calculated for C₂₀H₁₆N₂S₂, 349.0097). ¹H NMR (500 MHz, CDCl₃, 300 K): δ (ppm): 8.71 (s, 2H), 7.68 (d, *J* = 10 Hz, 4H), 7.54 (d, *J* = 10 Hz, 4H), 2.60 (s, 6H). ¹³C NMR (500 MHz, CDCl₃, 300 K), δ (ppm): 150.54, 148.87, 139.93, 131.65, 131.46, 129.90, 127.42, 16.37.

9,10-bis(4-methylthiazol-5-yl)anthracene (CD13). Pure product was obtained by precipitation method. *n*-hexane was added to a concentrated dichloromethane solution followed by filtering and washing with *n*-hexane. Light orange solid. Yield: 319.98 mg, 86%. MS (EI) *m/z* [M + H]⁺ = 373.0169 (calculated for C₂₂H₁₆N₂S₂, 373.0132). ¹H NMR (500 MHz, CDCl₃, 300 K): δ (ppm): 9.06 (s, 2H), 7.74 - 7.71 (m, 4H), 7.47 - 7.45 (m, 4H), 2.23 (s, 3H), 2.19 (s, 3H). ¹³C NMR (500 MHz, CDCl₃, 300 K), δ (ppm): 153.23, 153.20, 152.76, 152.66, 131.49, 126.54, 126.39, 15.61, 15.54.

Competition experiment. The comparison of the yields of the reactions of the 4-substituted thiazoles was done. The reaction conditions were identical to the one used above, but the reaction time was kept to eight hours. Both the thiazole and ethyl 4-thiazolecarboxylate had very small yields, so GCMS was used to determine the ratio of the biaryl compound and the aryl bromide.

Computational and Theoretical Methods. All calculations were performed with the Gaussian16 software package⁵⁵. Optimized structures of stationary points were illustrated with ChemCraft¹². Geometry optimizations were performed at the PBE0-D3(BJ)/def2-SVP level⁵⁶⁻⁵⁷⁻⁵⁸. Transition state structures were obtained using the intrinsic reaction coordinate⁵⁹⁻⁶⁰ (IRC) method. Frequency calculations were performed on all stationary points, no imaginary frequencies were observed for the minima, and a single imaginary frequency corresponding to the reaction coordinate was found for all transition states (TSs).

Dimethyl formamide solvation was calculated based on the gas-phase optimized structures with single point calculations at the PBE0-D3(BJ)/def2-TZVP level using the SMD⁸ implicit solvent model ($\epsilon = 37.219$). Condensed Fukui function calculations were obtained based on the PBE0/def2-SVP results using the Multiwfn¹⁵ package. Orbital composition analysis of 4-methylthiazole is carried out using Multiwfn¹⁵ program with the natural orbital method. The plot of the HOMO for 4-methylthiazole is performed by mapping the corresponding cube obtained on 0.005 a.u. electron density isosurface using ChemCraft software¹².

The Fukui function is a useful reactivity indicator that can predict chemical properties like regioselectivity, electrophilicity, and nucleophilicity. The Fukui function is defined as a partial derivative of the total electron density within a molecule with N number of electrons at the constant external potential $v(r)$:⁶¹⁻⁶⁷

$$f(r) = \left(\frac{\partial \rho(r)}{\partial N} \right)_{v(r)} \quad (1)$$

Two Fukui functions can take two forms $f^+(r)$ and $f^-(r)$ depending on the change in the electron density. The Fukui function after an addition of an electron in a molecule is represented as $f^+(r)$, and the change in the electron density after losing the electron is represented as $f^-(r)$. Mathematically, $f^+(r)$ and $f^-(r)$ in the condensed-to-atom form can be approximated by:⁶⁸

$$f^+(r) = \rho_{N+1} - \rho_N \quad (2)$$

$$f^-(r) = \rho_N - \rho_{N-1} \quad (3)$$

where ρ_N , ρ_{N+1} and ρ_{N-1} are the electron densities of the molecule with N , $N+1$ and $N-1$ electrons at a frozen molecular geometry, respectively. The local reactivity of atoms within a molecule can be compared using condensed $f^+(r)$ and $f^-(r)$ functions. A larger local $f^+(r)$ function on an atom denotes its larger susceptibility to a nucleophilic attack (or its electrophilicity). Similarly, a larger local $f^-(r)$ function denotes its larger susceptibility to an electrophilic attack (or its nucleophilicity).

ASSOCIATED CONTENT

Supporting Information

The data underlying this study are available in the published article and its Supporting Information.

Unit cell representation, crystal data, ¹H NMR, and ¹³C NMR spectra of ligands, and synthesized direct arylated compounds. The xyz structures of the complexes involved in the reaction paths and the Fukui cube files are available in the ESI.

Accession Codes

CCDC 2079553 contains the supplementary crystallographic data for this paper.

AUTHOR INFORMATION

Corresponding Author

Mihaela C. Stefan – Department of Chemistry and Biochemistry, University of Texas at Dallas, Richardson, Texas 75080, United States.
 orcid.org/0000-0003-2475-4635; Phone: 972-883-6581.
 Email: mihaela@utdallas.edu

G. Andrés Cisneros – Department of Chemistry and Biochemistry, University of Texas at Dallas, Richardson, Texas 75080, United States.
 Department of Physics, University of Texas at Dallas, Richardson, Texas 75080, United States.
 orcid.org/0000-0001-6629-3430; Phone: 972-883-2885.
 Email: andres@utdallas.edu

Notes

The authors declare no competing financial interest.

ACKNOWLEDGMENT

Financial support provided by the National Science Foundation (CHE-1609880 and CHE-1566059) and Welch Foundation (AT1740) is gratefully acknowledged. M.C.S. thanks the generous endowed chair support from the Eugene McDermott Foundation. We thank Dr. Gregory T. McCandless for collecting the crystal structure data. SC and GAC gratefully acknowledge computational time provided by the University of North Texas CASCaMs CRUNTCh3 high-performance cluster partially supported by NSF grant CHE-1531468 and XSEDE supported by project TG-CHE160044. We also acknowledge Dr. Tanay Debnath and Perouza Parsamian for suggestions on some computational analysis and aid in making the graphical abstract.

REFERENCES

- Blakemore, D. C.; Castro, L.; Churcher, I.; Rees, D. C.; Thomas, A. W.; Wilson, D. M.; Wood, A., Organic synthesis provides opportunities to transform drug discovery. *Nat. Chem.* **2018**, *10*, 383-394.
- Rossi, R.; Lessi, M.; Manzini, C.; Marianetti, G.; Bellina, F., Direct (Hetero)arylation Reactions of (Hetero)arenes as Tools for the Step- and Atom-Economical Synthesis of Biologically Active Unnatural Compounds Including Pharmaceutical Targets. *Synthesis* **2016**, *48*, 3821-3862.
- Mainville, M.; Leclerc, M., Direct (Hetero)arylation: A Tool for Low-Cost and Eco-Friendly Organic Photovoltaics. *ACS Appl. Polym. Mater.* **2020**, *3*, 2-13.
- Fell, V. H. K.; Findlay, N. J.; Breig, B.; Forbes, C.; Inigo, A. R.; Cameron, J.; Kanibolotsky, A. L.; Skabara, P. J., Effect of end group functionalisation of small molecules featuring the fluorene–thiophene–benzothiadiazole motif as emitters in solution-processed red and orange organic light-emitting diodes. *J. Mater. Chem. C* **2019**, *7*, 3934-3944.
- Meena, C. L.; Singh, P.; Shaliwal, R. P.; Kumar, V.; Kumar, A.; Tiwari, A. K.; Asthana, S.; Singh, R.; Mahajan, D., Synthesis and evaluation of thiophene based small molecules as potent inhibitors of Mycobacterium tuberculosis. *Eur. J. Med. Chem.* **2020**, *208*, 112772.
- Alberico, D.; Scott, M. E.; Lautens, M., Aryl–Aryl Bond Formation by Transition-Metal-Catalyzed Direct Arylation. *Chem. Rev.* **2007**, *107*, 174-238.

7. Zhao, Q.; Meng, G.; Nolan, S. P.; Szostak, M., N-Heterocyclic Carbene Complexes in C–H Activation Reactions. *Chem. Rev.* **2020**, *120*, 1981-2048.
8. Mercier, L. G.; Leclerc, M., Direct (Hetero)Arylation: A New Tool for Polymer Chemists. *Acc. Chem. Res.* **2013**, *46*, 1597-1605.
9. Song, A. X.; Zeng, X.-X.; Ma, B.-B.; Xu, C.; Liu, F.-S., Direct (Hetero)arylation of Heteroarenes Catalyzed by Unsymmetrical Pd-PEPPSI-NHC Complexes under Mild Conditions. *Organometallics* **2020**, *39*, 3524-3534.
10. Kumar, A.; Kumar, M.; Verma, A. K., Well-Defined Palladium N-Heterocyclic Carbene Complexes: Direct C–H Bond Arylation of Heteroarenes. *J. Org. Chem.* **2020**, *85*, 13983-13996.
11. Piou, T.; Slutskyy, Y.; Kevin, N. J.; Sun, Z.; Xiao, D.; Kong, J., Direct Arylation of Azoles Enabled by Pd/Cu Dual Catalysis. *Org. Lett.* **2021**, *23*, 1996-2001.
12. Tlahuext-Aca, A.; Lee, S. Y.; Sakamoto, S.; Hartwig, J. F., Direct Arylation of Simple Arenes with Aryl Bromides by Synergistic Silver and Palladium Catalysis. *ACS Catalysis* **2021**, *11*, 1430-1434.
13. Shi, X.; Sosa Carrizo, E. D.; Cordier, M.; Roger, J.; Pirio, N.; Hierso, J.-C.; Fleurat-Lessard, P.; Soulé, J.-F.; Doucet, H., C–H Bond Arylation of Pyrazoles at the β -Position: General Conditions and Computational Elucidation for a High Regioselectivity. *Chem. - Eur. J.* **2021**, *27*, 5546-5554.
14. Gandon, V.; Hoarau, C., Concerted vs Nonconcerted Metalation–Deprotonation in Orthogonal Direct C–H Arylation of Heterocycles with Halides: A Computational Study. *J. Org. Chem.* **2021**, *86*, 1769-1778.
15. Mohr, Y.; Alves-Favaro, M.; Rajapaksha, R.; Hisler, G.; Ranscht, A.; Samanta, P.; Lorentz, C.; Duguet, M.; Mellot-Draznieks, C.; Quadrelli, E. A.; Wisser, F. M.; Canivet, J., Heterogenization of a Molecular Ni Catalyst within a Porous Macroligand for the Direct C–H Arylation of Heteroarenes. *ACS Catal.* **2021**, *11*, 3507-3515.
16. Kaloğlu, M.; Kaloğlu, N.; Özdemir, İ., Palladium-PEPPSI-NHC Complexes Bearing Imidazolidin-2-Ylidene Ligand: Efficient Precatalysts for the Direct C5-Arylation of N-Methylpyrrole-2-Carboxaldehyde. *Catal. Lett.* **2021**, *151*, 3197-3212.
17. Xu, H.-F.; Pan, Y.-L.; Li, G.-J.; Hu, X.-Y.; Chen, J.-Z., Copper(II)-Catalyzed Direct C–H (Hetero)arylation at the C3 Position of Indoles Assisted by a Removable N,N-Bidentate Auxiliary Moiety. *J. Org. Chem.* **2021**, *86*, 1789-1801.
18. Amaladass, P.; Clement, J. A.; Mohanakrishnan, A. K., Pd-mediated C–H arylation of EDOT and synthesis of push–pull systems incorporating EDOT. *Tetrahedron* **2007**, *63*, 10363-10371.
19. Liu, C.-Y.; Zhao, H.; Yu, H.-h., Efficient Synthesis of 3,4-Ethylenedioxythiophene (EDOT)-Based Functional π -Conjugated Molecules through Direct C–H Bond Arylations. *Org. Lett.* **2011**, *13*, 4068-4071.
20. Jafarpour, F.; Rahiminejadan, S.; Hazrati, H., Triethanolamine-Mediated Palladium-Catalyzed Regioselective C-2 Direct Arylation of Free NH-Pyrroles. *J. Org. Chem.* **2010**, *75*, 3109-3112.
21. Karlinskii, B. Y.; Kostyukovich, A. Y.; Kucherov, F. A.; Galkin, K. I.; Kozlov, K. S.; Ananikov, V. P., Directing-Group-Free, Carbonyl Group-Promoted Catalytic C–H Arylation of Bio-Based Furans. *ACS Catal.* **2020**, *10* (19), 11466-11480.
22. Allard, S.; Forster, M.; Souharce, B.; Thiem, H.; Scherf, U., Organic semiconductors for solution-processable field-effect transistors (OFETs). *Angew. Chem., Int. Ed. Engl.* **2008**, *47*, 4070-98.
23. Koumura, N.; Wang, Z.-S.; Mori, S.; Miyashita, M.; Suzuki, E.; Hara, K., Alkyl-Functionalized Organic Dyes for Efficient Molecular Photovoltaics. *J. Am. Chem. Soc.* **2006**, *128* (4), 14256-14257.
24. Liu, X.-W.; Shi, J.-L.; Yan, J.-X.; Wei, J.-B.; Peng, K.; Dai, L.; Li, C.-G.; Wang, B.-Q.; Shi, Z.-J., Regioselective Arylation of Thiazole Derivatives at 5-Position via Pd Catalysis under Ligand-Free Conditions. *Org. Lett.* **2013**, *15*, 5774-5777.
25. Turner, G. L.; Morris, J. A.; Greaney, M. F., Direct Arylation of Thiazoles on Water. *Angew. Chem., Int. Ed.* **2007**, *46*, 7996-8000.
26. Boibessot, T.; Zschiedrich, C. P.; Lebeau, A.; Bénimèlis, D.; Dunyach-Rémy, C.; Lavigne, J.-P.; Szurmant, H.; Benfodda, Z.; Meffre, P., The Rational Design, Synthesis, and Antimicrobial Properties of Thiophene Derivatives That Inhibit Bacterial Histidine Kinases. *J. Med. Chem.* **2016**, *59*, 8830-8847.
27. Ouyang, J.-S.; Li, Y.-F.; Shen, D.-S.; Ke, Z.; Liu, F.-S., Bulky α -diimine palladium complexes: highly efficient for direct C–H bond arylation of heteroarenes under aerobic conditions. *Dalton Trans.* **2016**, *45*, 14919-14927.
28. Chen, F.-M.; Huang, F.-D.; Yao, X.-Y.; Li, T.; Liu, F.-S., Direct C–H heteroarylation by an acenaphthyl-based α -diimine palladium complex: improvement of the reaction efficiency for bi(hetero)aryls under aerobic conditions. *Org. Chem. Front.* **2017**, *4*, 2336-2342.
29. Roy, D.; Mom, S.; Royer, S.; Lucas, D.; Hierso, J.-C.; Doucet, H., Palladium-Catalyzed Direct Arylation of Heteroaromatics with Activated Aryl Chlorides Using a Sterically Relieved Ferrocenyl-Diphosphane. *ACS Catal.* **2012**, *2*, 1033-1041.
30. Yamaguchi, M.; Hagiwara, R.; Gayama, K.; Suzuki, K.; Sato, Y.; Konishi, H.; Manabe, K., Direct C3-Selective Arylation of N-Unsubstituted Indoles with Aryl Chlorides, Triflates, and Nonaflates Using a Palladium–Dihydroxyterphenylphosphine Catalyst. *J. Org. Chem.* **2020**, *85*, 10902-10912.
31. Zhang, Y.; Lee, J. C. H.; Reese, M. R.; Boscoe, B. P.; Humphrey, J. M.; Helal, C. J., 5-Aryltetrazoles from Direct C–H Arylation with Aryl Bromides. *J. Org. Chem.* **2020**, *85*, 5718-5723.
32. Li, Y.; Wang, J.; Huang, M.; Wang, Z.; Wu, Y.; Wu, Y., Direct C–H Arylation of Thiophenes at Low Catalyst Loading of a Phosphine-Free Bis(alkoxo)palladium Complex. *J. Org. Chem.* **2014**, *79* (7), 2890-2897.
33. Bhaskar, R.; Sharma, A. K.; Singh, A. K., Palladium(II) Complexes of N-Heterocyclic Carbene Amidates Derived from Chalcogenated Acetamide-Functionalized 1H-Benzimidazolium Salts: Recyclable Catalyst for Regioselective Arylation of Imidazoles under Aerobic Conditions. *Organometallics* **2018**, *37*, 2669-2681.
34. Okazawa, T.; Satoh, T.; Miura, M.; Nomura, M., Palladium-Catalyzed Multiple Arylation of Thiophenes. *J. Am. Chem. Soc.* **2002**, *124*, 5286-5287.
35. Matsidik, R.; Martin, J.; Schmidt, S.; Obermayer, J.; Lombeck, F.; Nübling, F.; Komber, H.; Fazzi, D.; Sommer, M., C–H Arylation of Unsubstituted Furan and Thiophene with Acceptor Bromides: Access to Donor–Acceptor–Donor-Type Building Blocks for Organic Electronics. *J. Org. Chem.* **2015**, *80*, 980-987.
36. Png, Z. M.; Tam, T. L. D.; Xu, J., Carboxylic Acid Directed C–H Arylation of Azulene. *Org. Lett.* **2020**, *22*, 5009-5013.
37. Türker, F.; Bereket, İ.; Barut Celepci, D.; Aktaş, A.; Gök, Y., New Pd-PEPPSI complexes bearing meta-cyanobenzyl-Substituted NHC: Synthesis, characterization, crystal structure and catalytic activity in direct C–H arylation of (Hetero)arenes with aryl bromides. *J. Mol. Struct.* **2020**, *1205*, 127608.

38. Hu, L.-Q.; Deng, R.-L.; Li, Y.-F.; Zeng, C.-J.; Shen, D.-S.; Liu, F.-S., Developing Bis(imino)acenaphthene-Supported N-Heterocyclic Carbene Palladium Precatalysts for Direct Arylation of Azoles. *Organometallics* **2018**, *37*, 214-226.
39. He, X.-X.; Li, Y.; Ma, B.-B.; Ke, Z.; Liu, F.-S., Sterically Encumbered Tetraarylimidazolium Carbene Pd-PEPPSI Complexes: Highly Efficient Direct Arylation of Imidazoles with Aryl Bromides under Aerobic Conditions. *Organometallics* **2016**, *35*, 2655-2663.
40. Canivet, J.; Yamaguchi, J.; Ban, I.; Itami, K., Nickel-Catalyzed Biaryl Coupling of Heteroarenes and Aryl Halides/Triflates. *Org. Lett.* **2009**, *11* (8), 1733-1736.
41. Hachiya, H.; Hirano, K.; Satoh, T.; Miura, M., Nickel-Catalyzed Direct C-H Arylation and Alkenylation of Heteroarenes with Organosilicon Reagents. *Angew. Chem., Int. Ed.* **2010**, *49*, 2202-2205.
42. Larson, H.; Schultz, D.; Kalyani, D., Ni-Catalyzed C-H Arylation of Oxazoles and Benzoxazoles Using Pharmaceutically Relevant Aryl Chlorides and Bromides. *J. Org. Chem.* **2019**, *84*, 13092-13103.
43. Hachiya, H.; Hirano, K.; Satoh, T.; Miura, M., Nickel-Catalyzed Direct Arylation of Azoles with Aryl Bromides. *Org. Lett.* **2009**, *11*, 1737-1740.
44. Zhao, S.; Liu, B.; Zhan, B.-B.; Zhang, W.-D.; Shi, B.-F., Nickel-Catalyzed Ortho-Arylation of Unactivated (Hetero)aryl C-H Bonds with Arylsilanes Using a Removable Auxiliary. *Org. Lett.* **2016**, *18*, 4586-4589.
45. Talukder, M. M.; Cue, J. M. O.; Miller, J. T.; Gamage, P. L.; Aslam, A.; McCandless, G. T.; Biewer, M. C.; Stefan, M. C., Ligand Steric Effects of α -Diimine Nickel(II) and Palladium(II) Complexes in the Suzuki-Miyaura Cross-Coupling Reaction. *ACS Omega* **2020**, *5* (37), 24018-24032.
46. Talukder, M. M.; Miller, J. T.; Cue, J. M. O.; Udamulle, C. M.; Bhadrans, A.; Biewer, M. C.; Stefan, M. C., Mono- and Dinuclear α -Diimine Nickel(II) and Palladium(II) Complexes in C-S Cross-Coupling. *Organometallics* **2021**, *40*, 83-94.
47. Mirabal, R. A.; Vanderzwet, L.; Abuadas, S.; Emmett, M. R.; Schipper, D., Dehydration Polymerization for Poly(hetero)arene Conjugated Polymers. *Chem. - Eur. J.* **2018**, *24*, 12231-12235.
48. Zhang, L.; Colella, N. S.; Cherniawski, B. P.; Mannsfeld, S. C. B.; Briseno, A. L., Oligothiophene Semiconductors: Synthesis, Characterization, and Applications for Organic Devices. *ACS Appl. Mater. Interfaces* **2014**, *6*, 5327-5343.
49. Yoshizawa, M.; Catti, L., Bent Anthracene Dimers as Versatile Building Blocks for Supramolecular Capsules. *Acc. Chem. Res.* **2019**, *52*, 2392-2404.
50. Pilepić, V.; Uršić, S., Nucleophilic reactivity of the nitroso group. Fukui function DFT calculations for nitrosobenzene and 2-methyl-2-nitrosopropane. *Journal of Molecular Structure: THEOCHEM* **2001**, *538* (1-3), 41-49.
51. *Chemical reactivity theory: a density functional view.* Chattaraj, P. K., Ed; CRC press: 2009.
52. Fuentealba, P.; Florez, E.; Tiznado, W., Topological analysis of the Fukui function. *Journal of chemical theory and computation* **2010**, *6* (5), 1470-1478.
53. Kavimani, M.; Balachandran, V.; Narayana, B.; Vanasundari, K.; Revathi, B., Topological analysis (BCP) of vibrational spectroscopic studies, docking, RDG, DSSC, Fukui functions and chemical reactivity of 2-methylphenylacetic acid. *Spectrochimica Acta Part A: Molecular and Biomolecular Spectroscopy* **2018**, *190*, 47-60.
54. Brala, C. J.; Fabijanić, I.; Marković, A. K.; Pilepić, V., The average local ionization energy and Fukui function of L-ascorbate, the local reactivity descriptors of antioxidant reactivity. *Computational and Theoretical Chemistry* **2014**, *1049*, 1-6.
55. Frisch, M. e.; Trucks, G.; Schlegel, H.; Scuseria, G.; Robb, M.; Cheeseman, J.; Scalmani, G.; Barone, V.; Petersson, G.; Nakatsuji, H., Gaussian 16. Gaussian, Inc. Wallingford, CT: 2016.
56. Adamo, C.; Barone, V., Toward reliable density functional methods without adjustable parameters: The PBE0 model. *J. Chem. Phys.* **1999**, *110* (13), 6158-6170.
57. Ernzerhof, M.; Scuseria, G. E., Assessment of the Perdew-Burke-Ernzerhof exchange-correlation functional. *J. Chem. Phys.* **1999**, *110* (11), 5029-5036.
58. Schäfer, A.; Horn, H.; Ahlrichs, R., Fully optimized contracted Gaussian basis sets for atoms Li to Kr. *The Journal of Chemical Physics* **1992**, *97* (4), 2571-2577.
59. Fukui, K., Formulation of the reaction coordinate. *The Journal of Physical Chemistry* **1970**, *74* (23), 4161-4163.
60. Chebbi, M.; Arfaoui, Y., Reactivity of pyrazole derivatives with halomethanes: A DFT theoretical study. *Journal of Molecular Modeling* **2018**, *24* (8), 1-10.
61. Fukui, K.; Yonezawa, T.; Shingu, H., A molecular orbital theory of reactivity in aromatic hydrocarbons. *The Journal of Chemical Physics* **1952**, *20* (4), 722-725.
62. Kohn, W.; Becke, A. D.; Parr, R. G., Density functional theory of electronic structure. *The Journal of Physical Chemistry* **1996**, *100* (31), 12974-12980.
63. Parr, R. G.; Yang, W., Density-functional theory of the electronic structure of molecules. *Annual review of physical chemistry* **1995**, *46* (1), 701-728.
64. Parr, R. G.; Weitao, Y., Chemical potential derivatives. In *Density-Functional Theory of Atoms and Molecules*, Oxford University Press: 1989.
65. Yang, W.; Parr, R. G., Hardness, softness, and the fukui function in the electronic theory of metals and catalysis. *PNAS*, **1985**, *82*, 6723-6726.
66. Geerlings, P.; De Proft, F., Conceptual DFT: the chemical relevance of higher response functions. *Physical Chemistry Chemical Physics* **2008**, *10*, 3028-3042.
67. Parr, R. G.; Yang, W., Density functional approach to the frontier-electron theory of chemical reactivity. *Journal of the American Chemical Society* **1984**, *106*, 4049-4050.
68. Mortier, W. J.; Ghosh, S. K.; Shankar, S., Electronegativity-equalization method for the calculation of atomic charges in molecules. *Journal of the American Chemical Society* **1986**, *108*, 4315-4320.
69. Sheldrick, G. M., SHELXT-Integrated Space-Group and Crystalstructure Determination. *Acta Crystallogr., Sect. A: Found. Adv.* **2015**, *71*, 3-8.
70. Sheldrick, G. M., Crystal Structure Refinement with SHELXL. *Acta Crystallogr., Sect. C: Struct. Chem.* **2015**, *71*, 3-8.
71. (a) Shibahara, F. and Murai, T., Direct C-H Arylation of Heteroarenes Catalyzed by Palladium/Nitrogen-Based Ligand Complexes. *Asian Journal of Organic Chemistry*, **2013**, *2*, 624-636. (b) Kaloglu, M. and Özdemir, İ., Palladium(II)-N-heterocyclic carbene-catalyzed direct C2- or C5-arylation of thiazoles with aryl bromides, *Tetrahedron*, **2018**, *74*, 2837-2845.
72. (a) G. W. Wheland, A Quantum Mechanical Investigation of the Orientation of Substituents in Aromatic Molecules, *J. Am. Chem. Soc.*, **1942**, *64*, 900 (b) Yang, Y-F, She, Y. Computational exploration of Pd-catalyzed C-H bond activation reactions. *Int J Quantum Chem.* **2018**; *118*:e25723. <https://doi.org/10.1002/qua.25723>
73. Park, C-H, Ryabova, V., Seregin, I., Seregin, V., Anna, W., and Gevorgyan, V., Palladium-Catalyzed Arylation

and Heteroarylation of Indolizines, *Organic Letters*, 2004, 6, 1159-1162.

74. Sinclair, G.S., Kukor, A.J., Imperial, K.K.G. and Schipper, D.J., Transition-Metal-Free ipso-Arylative Condensation. *Macromolecules*, 2020, 53, 5169-5176.